Synthesis of multilayer Nano-ZrO_2 coated polystyrene spheres on fabrication of three-dimensional ordered macroporous structures

YUJI HOTTA*, YU JIA, MIHARU KAWAMURA, NAOKI OMURA, KIYOKA TSUNEKAWA, KIMIYASU SATO, KOJI WATARI
National Institute of Advanced Industrial Science and Technology (AIST), Anagahora 2266-98, Shimoshidami, Moriyama-ku, Nagoya 463-8560, Japan
E-mail: y-hotta@aist.go.jp

Published online: 9 March 2006

Monodispersed ZrO_2 precursor nanoparticles with a diameter of 25 nm were successfully synthesized by using diglycol as complexing reagent. The kinetic of particle growth as a function of concentration ratio of $ZrOCl_2$: diglycol was investigated. The as-synthesized ZrO_2 precursor nanoparticles were homogenously coated on the surface of polystyrene particles. Multilayer coating process was implemented by using poly (acrylic acid) (PAA) to modify the surface charges of the coated spheres, which was characterized by zeta-potential, particles size distribution and microstructural observation. The multilayer-coated polystyrene (PS) spheres have been used as templates to produce macroporous materials. Ordered macroporous ZrO_2 materials were obtained after the ZrO_2 precursor nanoparticles coated PS spheres were formed by centrifugation and calcined at 550°C for 3 h. The porous wall thickness could be well controlled by using the multilayer nano-ZrO_2 coated PS spheres with different coating thickness.

1. Introduction

Porous ceramics have a number of important applications in devices that include filters, bioceramics, fuel-cell electrodes, membrane reactors, catalytic supports and surfaces, and optical devices [1–3]. In fact, numerous properties of macroporous materials, such as density, thermal conductivity, and dielectric permittivity, are mainly dependent on their pore morphology (e.g. pore size, wall thickness, and structures) [4–7]. In the last decades, macroporous materials with tight control over the pore size distribution and porosity attracted a lot of interesting because of their unique optical, photonic and electrochemical properties [8–10]. On the other hand, macroporous ZrO_2 material is a potential application as electromagnetics and isomerizations [11, 12]. Furthermore, Y_2O_3-stabilized ZrO_2 can be used in solid oxide fuel cells (SOFC), which operate at high temperature [13–16].

At present, various methods have been developed for preparing ordered macroporous materials. Though ordered microstructure can be achieved by emulsion templating method, it is difficult to improve the porosity [17–19]. Colloidal crystal templating method using close-packed arrays of monodispersed spheres (polystyrene or silica) as templates have been developed to prepare three dimensionally ordered macroporous (3-DOM) materials that include silica [20, 21], metals [10, 22, 23], metal oxides [6, 24, 25], polymers [26] and carbon [27]. Nevertheless, control of porous wall thickness has been limited. On the other hand, ordered porous structures with a controlled pore size can be developed by colloidal templating method using pre-coated templates, and the porous wall thickness could be controlled by using templates with different coating thickness [28, 29].

One approach at the forefront in coating process research is the layer-by-layer (LbL) assembly method [30, 31]. However, the widely used starting materials were alkoxides that required for organic solvent. Since yttrium alkoxides precursor has limited solubility in zirconium alkoxides, it is difficult to prepare Y_2O_3-stabilized ZrO_2 materials [21].

*Author to whom all correspondence should be addressed.
0022-2461
DOI: 10.1007/s10853-006-6200-0

On the other hand, monodispersed nanoparticles have an advantage in fabrication of ceramics with improved properties: sintering, mechanical, electrical, thermal, ionic conductivity, catalytic, and optical [32–36]. However, nano-powder has property of strong aggregation because of the high surface energy. Therefore, prevention of the aggregation of nanoparticles is of importance for nano-materials research.

In the present work, we demonstrate how monodispersed nano-ZrO_2 (includes Y_2O_3) particles can be synthesized in aqueous solution by utilizing $ZrOCl_2$ and YCl_3 as starting materials. A novel route for homogenously coating of nano-ZrO_2 particles on the surface of polystyrene (PS) spheres surface was developed. The effect of the hydrolysis behavior of $ZrOCl_2$ on the morphology of nano-ZrO_2 particles coated PS spheres was studied. Moreover, it is shown how nano-ZrO_2 particles coated PS spheres can be used for preparing ordered ZrO_2 macroporous materials. Control of the porous wall thickness by utilizing pre-coated temples with different coating thickness was investigated.

2. Experimental section

2.1. Materials

Zirconium oxychloride ($ZrOCl_2{\cdot}8H_2O$, 98%) and tetraethyl orthosilane ($Si(OC_2H_5)_4$, TEOS) were obtained from Sigma-Aldrich Chemical Company. Polystyrene (PS) suspensions modified with sulfate functional group (concentration of 8 wt%, a particles size of 500 nm (1PS) and 1 μm (2PS)) were purchased form Interfacial Dynamics Corporation (Tualatin, USA). Polyacrylic acid (PAA, M_w 5000), $YCl_3{\cdot}6H_2O$ (99.9%), diglycol and reagent-grade sodium hydroxide (NaOH), hydrochloric acid (HCl) and sodium chloride (NaCl) were provided from Wako Pure Chemical Industry, Japan. All the reagents were used as received.

2.2. Synthesis of nano-ZrO_2 particles and coating method

In order to study the effect of hydrolysis behavior on coating of ZrO_2 precursor, three coating routes were performed: (1) directly coating of ZrO_2 particles (1PS/Zr), (2) coating of ZrO_2-SiO_2 composite particles (1PS/Zr-Si), and (3) coating of ZrO_2 particles in the presence of diglycol on 500 nm PS (1PS) spheres (1PS/Zr-DG).

For synthesizing 1PS/Zr particles, zirconium oxyhydrate solution was prepared by hydrolysis of 0.05 M $ZrOCl_2$, which contained YCl_3, in distilled water. The solution was diluted to 5×10^{-3} M after stirring for 48 h. Later, 40 ml of the diluted solution was mixed with 2 ml PS suspension and vigorously stirred for 72 h. 1PS/Zr-Si particles were prepared as the follows: 36 ml hydrolyzed $ZrOCl_2$ (5×10^{-3} M) was adjusted to pH 2 with HCl, and 4 ml ethanol was added. Then, 0.5 ml TEOS was introduced. After stirring for 1 h, 2 ml PS suspension was added and reacted for 72 h by vigorously stirring. In the case to prepare 1PS/Zr-DG particles, 150 ml hydrolyzed $ZrOCl_2$ (0.05 M), which contained YCl_3 (4.5×10^{-3} M), was mixed with 100 ml diglycol by vigorous magnetic stirring for 8 h. Later, the pH of the solution was adjusted to 5. After standing for 16 h, 5 ml PS suspension was dropped and stirred for 72 h. All the reacted suspensions of the 1PS/Zr, 1PS/Zr-Si and 1PS/Zr-DG particles were separated via centrifugation and the solids were washed with distilled water for 3 times.

Furthermore, coating of nano-ZrO_2 particles in the presence of diglycol (ZrO_2-DG particles) on 1 μm PS (2PS) spheres was carried out according to the same process as for preparing 1PS/Zr-DG particles. The one layer ZrO_2-DG particle coated PS spheres (2PS/1Zr-DG) was dispersed into 100 ml 0.03 M NaCl solution to make an electric double layer be stable at pH 4 and aged for 4 h. At the same time, 100 ml PAA solution (0.6 wt% in 0.03 M NaCl solution) was adjusted to pH 4 and aged for 4 h. Then, the PAA solution was added into the suspension and stirred for 15 h. The suspension was separated and the solid was washed by distilled water to remove the excess PAA. The PAA adsorbed particles (2PS/1Zr-DG /PAA) were deposited with ZrO_2-DG nanoparticles to get two layers of nano-ZrO_2 coated PS spheres (2PS/2Zr-DG). Table I shows the compositions of all the samples.

TABLE I Composition of the samples

Samples	Shell materials	Diameter of PS spheres (nm)
1PS	–	500
1PS/Zr	ZrO_2 precursor	500
1PS/Zr-Si	ZrO_2-SiO_2 precursor	500
1PS/Zr-DG	ZrO_2-DG precursor	500
2PS	–	1000
2PS/1Zr-DG	ZrO_2-DG precursor	1000
2PS/2Zr-DG	ZrO_2-DG precursor	1000

The compacts of 2PS/1Zr-DG and 2PS/2Zr-DG particles were formed by centrifugation. After drying in air, the compacts were calcined at 550°C for 3 h with a heating and cooling rate of 100°C /h.

2.3. Kinetics on nano-ZrO_2 particles from $ZrOCl_2$ solution

Zirconium oxyhydrate solution at two concentrations (0.02 M and 0.05 M), which contained YCl_3 (1.8×10^{-3} M and 4.5×10^{-3} M), were prepared by hydrolysis of $ZrOCl_2$ and YCl_3 in distilled water. Then, diglycol were added to the as-prepared solutions during vigorous magnetic stirring. 0.02 M $ZrOCl_2$ solutions were mixed with diglycol at the concentration ratio of 5:1, while 0.05 M $ZrOCl_2$ solutions were mixed with diglycol at the volume ratio of 1:1, 3:2 and 2:1, respectively. The pH of the mixtures was adjusted to 5 after the mixed source was aged for 8 h. After ageing from 4 to 360 h, the particle size of the synthesized nano-ZrO_2 was measured using

dynamic light scattering spectorophotometer (DLS-7600, Otsuka Electronics Co., Ltd., Japan).

2.4. Characterization

Morphology of the synthesized nano-ZrO_2 particles was observed using a transmission electron microscope (TEM, JEM-2010, JEOL, Japan). The zeta-potential of 2PS, 2PS/1Zr-DG, 2PS/1Zr-DG/PAA and 2PS/2Zr-DG particles was characterized using a microscope electrophoresis analyzer (Model 502, Nihon Rufuto Co., Ltd, Japan) in a 0.01 M NaCl solution and aged for 1 h. The particle size distributions of 2PS, 2PS/1Zr-DG and 2PS/2Zr-DG particles dispersed in distilled water were analyzed with a laser scattering particle size distribution analyzer (LA-920, Horiba, Japan). Scanning electron microscope (SEM, Model JSM5600N, JEOL, Japan) was used to observe the microstructure and morphology of the particles and calcined bodies. The existence of Zr, Si and Y components in powders was detected with an EDX apparatus (EDAX, DX-4, Netherlands). Thermo-gravimetric (TG) analysis was conducted under flowing air using a thermo-gravimetric instrument (RTG320, Seiko Instruments, Japan) at a heating rate of 3°C/min.

3. Results and discussion

Fig. 1 shows the SEM micrographs of 1PS, 1PS/Zr, 1PS/Zr-Si and 1PS/Zr-DG. The particle size estimated from the SEM micrographs was shown in Table II. The ZrO_2-SiO_2 composite is supported by EDX data of the 1PS/Zr-Si powders (Fig. 2). The 1PS/Zr particles have a broad particle size distribution between 525 and 741 nm. The 1PS/Zr-Si and 1PS/Zr-DG particles have an average diameter of 559 ± 13 nm and 548 ± 12 nm, respectively; hence the PS spheres have been coated with the nanoparticles. The relative monodispersity of the 1PS/Zr-Si (Fig. 1c) and 1PS/Zr-DG particles (Fig. 1d) indicates that the coating is uniform.

When directly coating PS spheres with hydrolyzed $ZrOCl_2$ is taken place, the related reactions can be represented as equations (1) and (2) [37]:

$$4ZrOCl_2 + 20H_2O \rightarrow [Zr_4(OH)_8(H_2O)_{16}Cl_6]^{2+} + 2Cl^- \quad (1)$$

$$2n[Zr_4(OH)_8(H_2O)_{16}Cl_6]^{2+} \rightarrow Zr_{8n}(OH)_{20n}(H_2O)_{24n}Cl_{12n} + 4nH_2O + 4nH^+ \quad (2)$$

The reactions are composed of hydrolysis (1) and nanocluster (2). Due to the fast hydrolysis and nanocluster, nucleation and growth were completed soon. Therefore,

TABLE II Diameter and film thickness of coated particle

Samples	Diameter of coated particle (nm)	Coating thickness (nm)
1PS	501 ± 4	–
1PS/Zr	$525 \sim 741$	$13 \sim 121$
1PS/Zr-Sr	559 ± 13	29
1PS/Zr-DG	548 ± 12	24

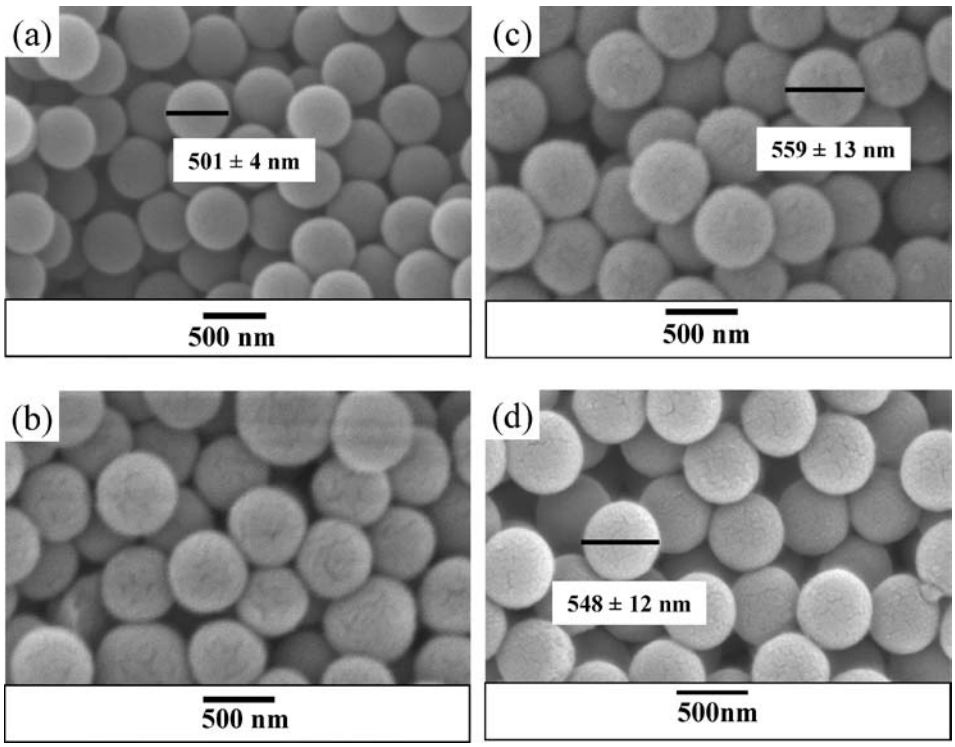

Figure 1 SEM micrographs of nano-particles coated PS spheres. (a) 1PS, (b) 1PS/Zr, (c) 1PS/Zr-Si, and (d) 1PS/Zr-DG particles.

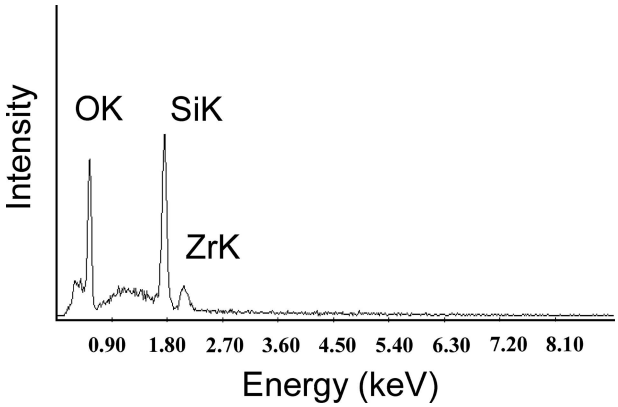

Figure 2 EDX spectrum of 1PS/Zr-Si particles.

the formed ZrO_2 precursor particles were unstable and easy to aggregate, which caused the coated PS spheres have a broad particle size. Hence, a stable and homogenous sol of ZrO_2 precursor nanoparticles is required for homogenous coating. Complexation is widely used to modify the sol-gel process, which slows down the hydrolysis and condensation rate [38,39]. In case of 1PS/Zr-Si particles, the ZrO_2 precursor sol was modified by TEOS. According to our previous work [28], homogenous coating of silica on PS spheres was performed using TEOS as the shell material. When TEOS is slowly hydrolyzed and condensated in water at pH 2, the reactions can be represented as follows:

$$\equiv \text{Si–OR} + \text{H}_2\text{O} \rightarrow \equiv \text{Si–OH} + \text{ROH} \quad (3)$$

$$\equiv \text{Si–OH} + \text{HO–Si} \equiv \rightarrow \equiv \text{Si–O–Si} \equiv + \text{H}_2\text{O} \quad (4)$$

Thus, when the hydrolyzed $ZrOCl_2$ and TEOS are mixed, co-condensation reactions are occurred as shown in the following equations:

$$\equiv \text{Zr–OH} + \text{HO–Si} \equiv \rightarrow \equiv \text{Zr–O–Si} \equiv + \text{H}_2\text{O} \quad (5)$$

$$\equiv \text{Zr–OH} + \text{RO–Si} \equiv \rightarrow \equiv \text{Zr–O–Si} \equiv + \text{ROH} \quad (6)$$

$$\equiv \text{Zr–OR} + \text{HO–Si} \equiv \rightarrow \equiv \text{Zr–O–Si} \equiv + \text{ROH} \quad (7)$$

Due to reactions (5) to (7), the condensation of ZrO_2-SiO_2 composite precursors is retrained. Therefore, a stable sol of ZrO_2-SiO_2 composite precursor nanoparticles is produced, which lead to the homogenous coating.

In case of diglycol used as a complex reagent, diglycol molecular reacts with $ZrOCl_2$ hydrolysis when the two liquids are mixed. The reactions can be represented as equations (8) to (10) [38, 39]:

$$\text{ZrOCl}_2 + \text{H}_2\text{O} + \text{XOH} \rightarrow \text{XO} - \text{Zr} \equiv + \text{HCl} \quad (8)$$

$$\text{XO–Zr} \equiv + \text{H}_2\text{O} + \text{XOH} \rightarrow (\text{XO})_n\text{Zr}(\text{OH})_{4-n} \quad (9)$$

$$(\text{XO})_n Zr(\text{OH})_{4-n} + (\text{HO})_{4-n}\text{Zr}(\text{OX})_n \rightarrow (\text{XO})_n(\text{OH})_{3-n}\text{Zr–O–Zr}(\text{OH})_{3-n}(\text{XO})_n + \text{H}_2\text{O} \quad (10)$$

where X represents $HO(CH_2)_2O(CH_2)_2$ functional group. The actual chemical process in the sol is much more complicate than those simplified by equations (8) to (10). The hydrolysis of chelated zirconium species is reduced due to steric effect. Furthermore, diglycol strongly restrain condensation of $ZrOCl_2$ as well as the hydrolysis, which inducing nucleation at the early stage of the sol-gel process. Hence, highly stable, monodispersed ZrO_2 precursor nanoparticles were prepared. Therefore, the coated PS spheres have a homogenous morphology. In addition, the as-synthesized ZrO_2-DG nanoparticles can be well dispersed in aqueous solution because of the surface modification of the hydroxyl group.

Fig. 3a shows the relationship between the reaction time and the particle size as a function of $ZrOCl_2$ concentration, at which the concentrations ratio of $ZrOCl_2$: diglycol is fixed to 5:1 for 0.02 M $ZrOCl_2$ solution and 2:1 for 0.05 M $ZrOCl_2$ solution on purpose of investigating the kinetic of particle growth at same mole ratio of $ZrOCl_2$: diglycol. The plots show the particle size parabolically with an initial rapid growth with time and an asymptotic approach to a maximum diameter. The growth of the particle size, δ, could be fitted by simple equation (11) describing the homogeneous particle growth kinetics [40],

$$\delta = \delta_M(1 - e^{-\kappa t}) \quad (11)$$

where δ_M is the maximum particle size, κ is the rate constant dictated by the solution condition, and t is the reaction time. After fitting to equation (11), the δ_M and κ can be estimated and are shown in Fig. 3b. It is seen that the maximum particle size and the rate constant increase with increasing the $ZrOCl_2$ concentration. Zukoski *et al*. reported the kinetics of the growth of uniform silica particles from silica precursor [40]. One important observation was that the silica particles grew by a surface limited mechanism. This observation is likely to hold true for our system as well. Fig. 3c shows the particle size growth kinetic as a function of the ratio of $ZrOCl_2$: diglycol for 0.05 M $ZrOCl_2$ solution. The δ_M and κ can be estimated that the maximum particle size and the rate constant increase when relatively lower content of diglycol was applied. It is well known that the sol-gel method is a versatile technique used to obtain ultrafine, homogenous powders of a variety of glass and ceramic materials at low temperature and in short time through the growth of metal oxo-polymers in a solvent. However, the hydrolysis and condensation involved in sol-gel process are generally fast and need to be inhibited to avoid precipitation. Likewise, electrolytes could affect the hydrolysis and condensation kinetics. In the present study, as chelated with diglycol, the precipitation rate was changed. The controlled sol-gel

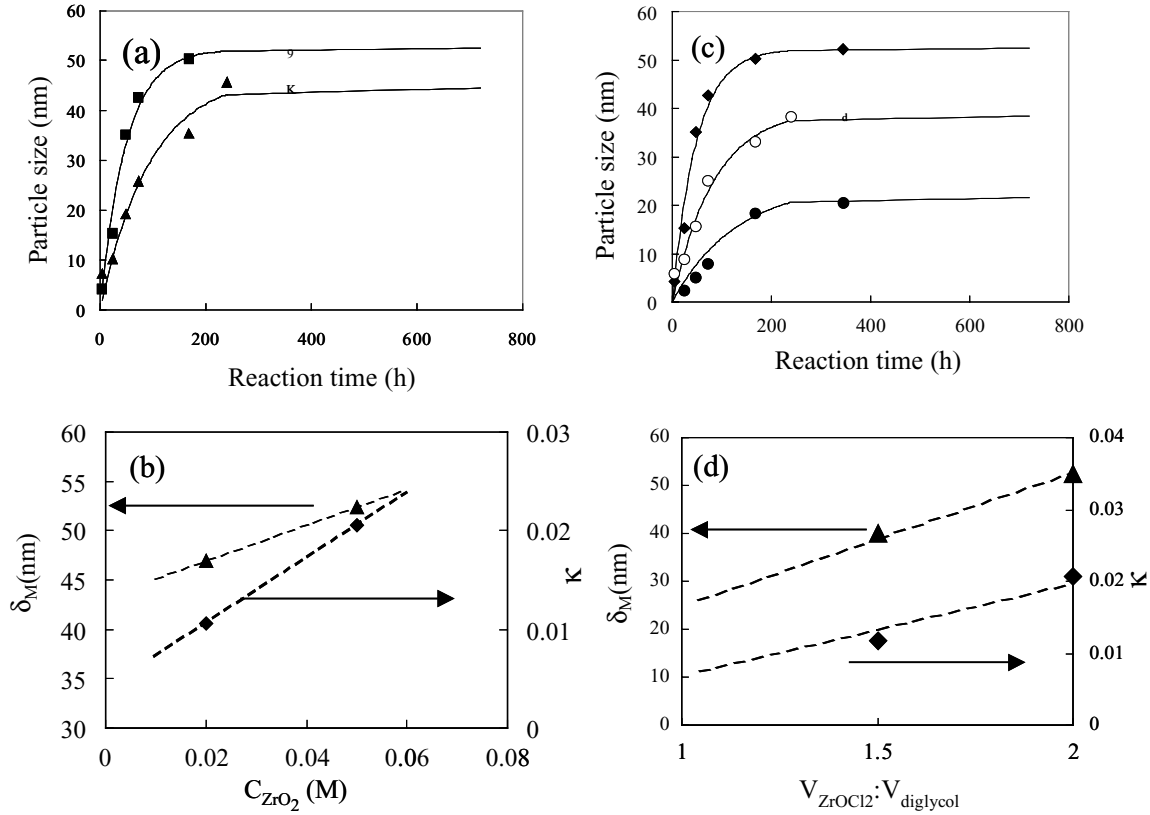

Figure 3 (a) Particle size growth as a function of reaction time at different concentrations of $ZrOCl_2$ solution (■0.05 M, ▲0.02 M), (b) final growth size of particles (δ_M) and rate constant (κ) at different concentration, (c) particle growth as a function of reaction time for 0.05 M $ZrOCl_2$ solution at different volume ratios of $ZrOCl_2$: diglycol (●1 : 1, ○3 :2, ◇2 :1), (d) final growth size of particles (δ_M) and rate constant (κ) at different concentration ratios of $ZrOCl_2$: diglycol.

process was described as equations (8) to (11). In the case that relatively low ratio of $ZrOCl_2$: diglycol has been used, the hydrolysis of the precursor was relatively slow due to the much more stable chelated structure. Therefore, the nucleation and growth of the particles were slow. As a result, the rate constant of the particle growth, κ, decrease with increasing the relative content of diglycol due to the chelating reactions. Hence, highly stable, monodispersed nano-ZrO_2 particles with controllable particle size were prepared. Besides, lower ratio of $ZrOCl_2$: diglycol means there are much higher chelated zirconium remained in the mixture after reaction. Therefore, the concentration of the nucleates is lower, which results in lower collision probability, and in turn, smaller final particle size.

Fig. 4 shows the TEM micrograph of the as-synthesized nano-ZrO_2 particles after 0.05 M $ZrOCl_2$ solution chelated with diglycol at a ratio of 3:2 was reacted for 72 h. It is observed from Fig. 4a that the particles have a monodispersed size of ca. 25 nm, which is in good agreement with the results of particle size in Fig. 3c. Fig. 4b shows a HRTEM image with the corresponding power spectrum (the square of the Fourier transform of the TEM image). It is determined that the particles are crystalline in the tetragonal structure without the presence of defaults. The distance between lattice planes that calculated from power spectrum is about 3×10^{-10} m. The faced particle is parallel to the (111) plane when a crystal lattice unit cell parameters $a = 0.512$ nm and $c = 0.525$ nm was selected [41]. On considering that the 1PS/Zr-DG particles have a coating thickness of 24 nm (shown in Table II), the 1PS particles was homogenously coated with single layer of ZrO_2-DG nanoparticles. Therefore, it was indicated that homogenously coating of ZrO_2-DG nanoparticles on PS spheres surface could be prepared by control of the hydrolysis and condensation behavior of $ZrOCl_2$.

Fig. 5 shows the zeta potential of 2PS, 2PS/1Zr-DG, 2PS/1Zr-DG/PAA, 2PS/2Zr-DG and ZrO_2-DG particles as a function of pH. 2PS particles surface was negatively charged throughout the measured pH region because of the modification of sulfate functional groups. The IEP of ZrO_2-DG particles were 6.6. PS spheres have high negative charge at pH 5, and the ZrO_2-DG nanoparticles has high positive charge. When the two suspensions were mixed, the ZrO_2-DG nanoparticles were homogenously deposited on PS spheres by heterocoagulation process due to the electrostatic attraction. The IEP of the coated particles (2PS/1Zr-DG) was 5.6. The IEP value was similar with the one of ZrO_2-DG particles, which means that PS spheres surface were covered with ZrO_2-DG nanoparticles. After PAA was adsorbed on the surface of 2PS/1Zr-DG particles (2PS/1Zr-DG/PAA), the IEP was shifted from 5.6 to 2.4, which insure the follow-

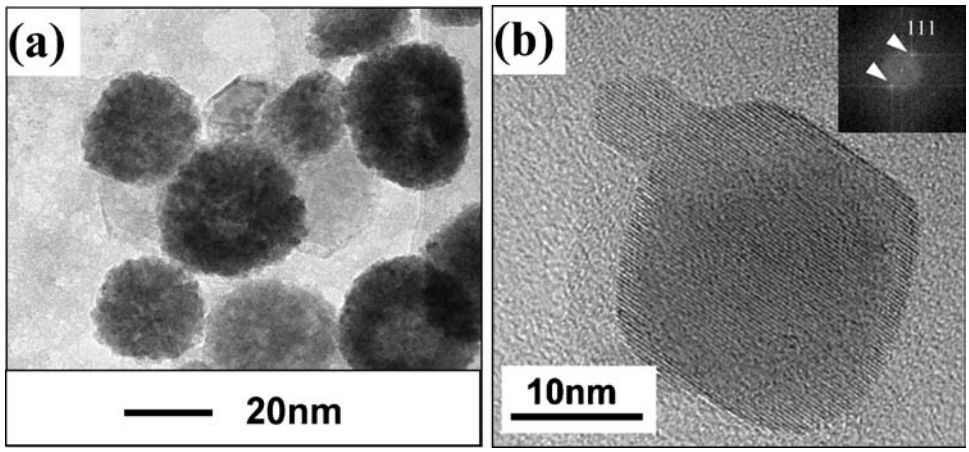

Figure 4 TEM micrographs. (a) As-synthesized particles from 0.05 M $ZrOCl_2$ mixed diglycol at a volume ratio of 3:2 for 72 h. (b) HRTEM image with the corresponding power spectrum.

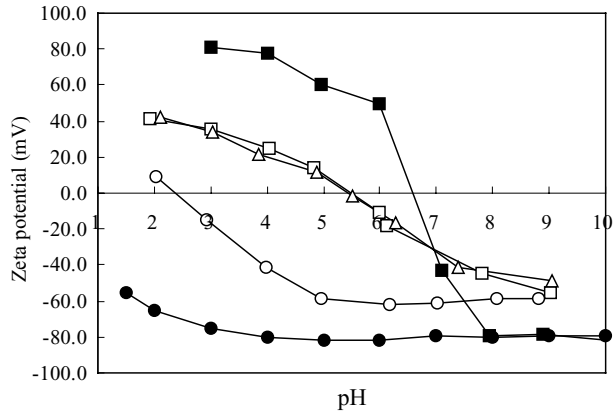

Figure 5 Zeta-potential plots of 2PS (filled circles), 2PS/1Zr-DG (open squares), 2PS/1Zr-DG/PAA (open circles), 2PS/2Zr-DG (open triangles) and ZrO_2-DG nanoparticles (filled squares).

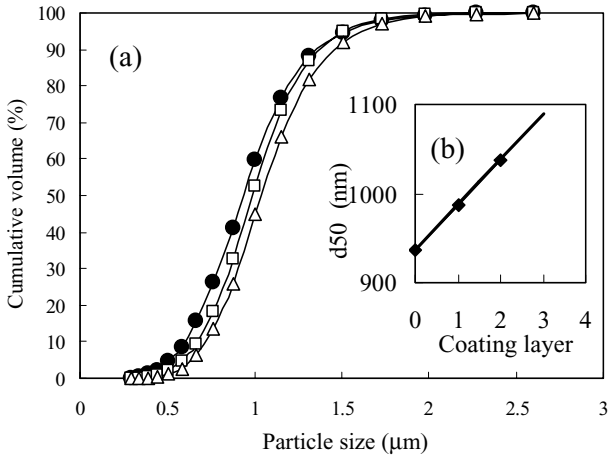

Figure 6 (a) Particle size distributions of 2PS (filled symbols), 2PS/1Zr-DG (open squares), and 2PS/2Zr-DG particles (open triangles); (b) d_{50} of particles coated with different layer of ZrO_2-DG nanoparticles.

ing coating of ZrO_2-DG nanoparticles on the particles surface. The zeta potential plot of 2PS/2Zr-DG particles was identified with the one of 2PS/1Zr-DG particles. Therefore, it was indicated that the multilayer-coated PS particles could be synthesized by repeating the ZrO_2-DG deposition and PAA adsorption steps indefinitely to get required coating thickness.

Fig. 6 shows the particle size distribution (Fig. 6a) and d_{50} (Fig. 6b) of 2PS, 2PS/1Zr-DG, and 2PS/2Zr-DG particles. Each d_{50} of 2PS, 2PS/1Zr-DG and 2PS/2Zr-DG particles was 936 nm, 987 nm and 1038 nm, respectively. The particle size of 50 nm was increased by deposition of one time. Thus, the coating thickness of one layer was ca. 25 nm. It was indicated that 2PS/1Zr-DG and 2PS/2Zr-DG particles were homogenously coated with single layer and two layers of ZrO_2-DG nanoparticles, respectively, on considering that the ZrO_2-DG nanoparticles have a diameter of 25 nm. The SEM micrographs of 2PS, 2PS/1Zr-DG, and 2PS/2Zr-DG particles were shown in Fig. 7. The average particle sizes of 2PS/1Zr-DG and 2PS/2Zr-DG, which were estimated from the SEM macrographs, were 1053 and 1105 nm, respectively. The coating thickness of one layer was 26 nm. It was observed that ZrO_2-DG nanoparticles were homogenously coated on the PS spheres surface. This was agreed with the nanoparticle size estimated from the TEM micrograph (Fig. 4) and the particles size distribution (Fig. 3 and Fig. 6).

Fig. 8 shows TG curves of 2PS, 2PS/1Zr-DG and 2PS/2Zr-DG particles. TG curve of 2PS spheres indicated that 2PS spheres were decomposed from 250°C to 400°C. 2PS/1Zr-DG particles have a slight weight loss bellow 275°C due to the evaporation of absorbed water and residual diglycol, and dehydration of Zr-OH to ZrO_2. PS spheres were decomposed from 275°C. The weight loss occurred from 325°C to 500°C was caused by crystallization of Zr-OR into ZrO_2 [42] and the decomposition of the residual PS spheres. For 2PS/2Zr-DG particles, the decomposition of PS spheres started at 300°C. There was a radical increasing of the temperature from 350°C to 400°C, after then the temperature was decreased to 370°C again. After coated with two layers of ZrO_2-DG nanoparticles, the coating thickness was increased. As a result,

releasing of hot gas that resulted from the PS spheres decomposition was slow down, which caused in the radical increasing of the temperature. When the hot gas was released and most of the PS spheres were decomposed, the sample was cool down a little. Above 500°C, there was no apparent weight loss for all of the three particles, which indicated that 550°C was a suitable calcinations temperature. Due to the coating of ZrO_2-DG, the beginning decomposition temperature of PS spheres was increased a little compared to the uncoated PS spheres. Furthermore, it could be calculated from the TG curves that 2PS/1Zr-DG and 2PS/2Zr-DG particles contained 13 wt% and 30 wt% ZrO_2-DG nanoparticles, respectively.

Fig. 9 shows the SEM micrographs of 2PS/1Zr-DG and 2PS/2Zr-DG calcined bodies. It could be observed that macroporous materials with ordered microstructure and connected channels were obtained after the compacts were calcined. From the TG curves, we found that

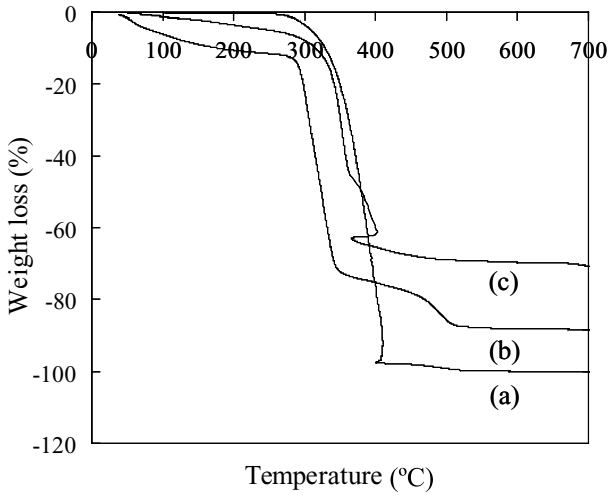

Figure 8 TG curves of (a) 2PS, (b) 2PS/1Zr-DG, and (c) 2PS/2Zr-DG particles.

the 2PS/1Zr-DG and 2PS/2Zr-DG particles have a slight weight loss upon to 275°C and 300°C, respectively, which was result from the evaporation of absorbed water and residual diglycol, and dehydration of Zr-OH to ZrO_2. Due to the evaporation and dehydration, the coated nanoparticles connected to each other, which preserved the ordered macroporous structure without collapsed after PS spheres were decomposed. Furthermore, it could be observed that the porous wall thickness of the calcined bodies obtained from 2PS/1Zr-DG particles was thinner than the one from

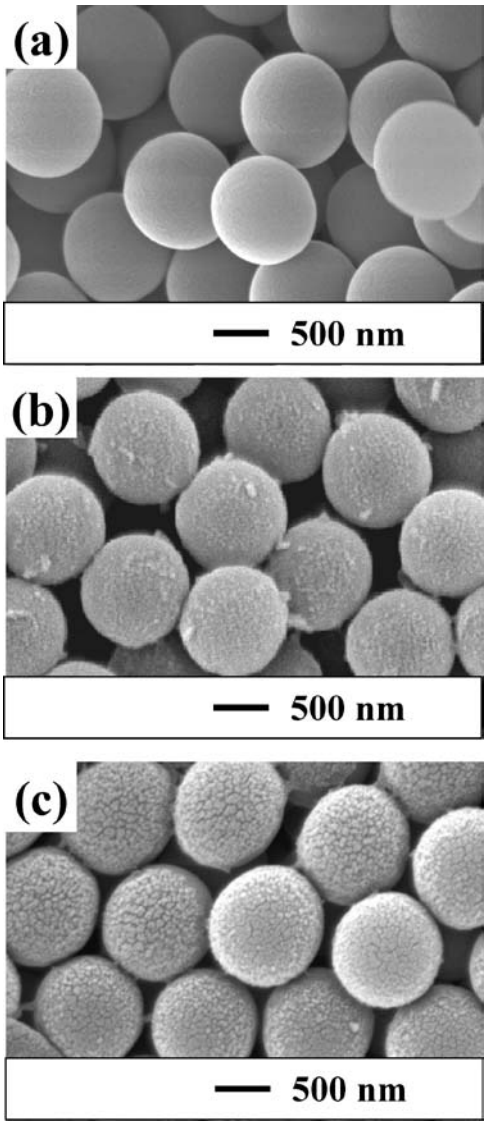

Figure 7 SEM micrographs of (a) 2PS, (b) 2PS/1Zr-DG, and (c) 2PS/2Zr-DG particles.

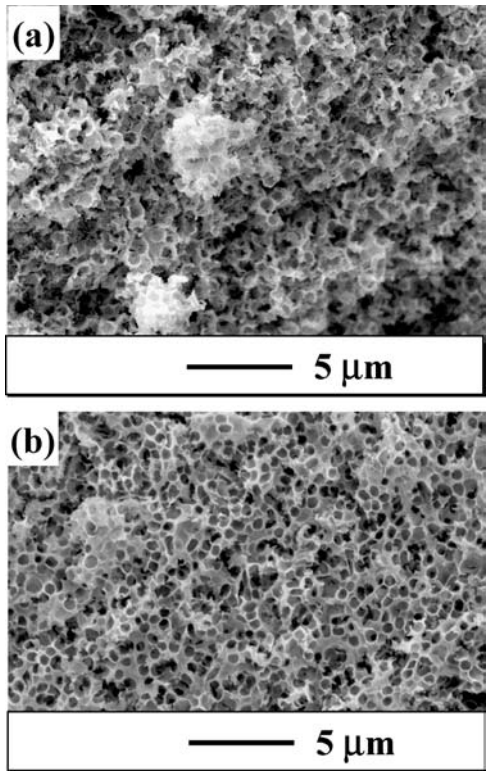

Figure 9 SEM micrographs of (a) 2PS/1Zr-DG, and (b) 2PS/2Zr-DG calcined bodies.

2PS/2Zr-DG particles. Therefore, it was indicated that the porous wall thickness of the final macroporous materials could be controlled by utilizing pre-coated temples particles with different coating thickness.

4. Conclusions

The hydrolysis and condensation behavior of $ZrOCl_2$ was well controlled by utilizing diglycol as a complex reagent. As a result, 25 nm ZrO_2-DG nanoparticles, which could be dispersed in an aqueous solution, were synthesized when 0.05 M $ZrOCl_2$ solution mixed with diglycol at a concentration ratio of 3:2 and then reacted for 72 h. Moreover, ZrO_2-DG nanoparticles were homogenously coated on PS spheres surface. Multilayer-coated PS spheres with different coating thickness were produced using PAA to modify the surface charges of ZrO_2-DG coated particles. One layer and two layers shell coated particles have a coating thickness of 25 nm and 51 nm, and a ZrO_2-DG content of 13 wt% and 30 wt%, respectively. After ZrO_2-DG nanoparticles coated PS spheres were formed by centrifugation and calcined at 550°C, macroporous materials with ordered microstructure were obtained.

The present research provides a potential route for preparing dispersed nanoparticles from metal salts by using complex reagent to control the raw materials hydrolysis and condensation behavior. Furthermore, it is indicated that a possible application of nanoparticles as nanocomposites materials is to coat the dispersed nanoparticles on the surface of submicrometer or micrometer particles surface.

Acknowledgment

The authors thank Dr. S. Kume, AIST, for the support and keen interest in this work.

References

1. K. ISHIZAKI, S. KOMARNENT and M. NAURO, "Porous Materials Process Technology and Applications", (Kluwer, London, U.K. 1998).
2. M. HAROLD, C. LEE, A. J. BURGGRAAF, K. KEIZER, V. T. ZASPALLS and R. S. A. DE LANGEANGE, *Mater. Res. Soc. Bull.* **19** (1994) 34.
3. J. E. G. J. WIJMHOVEN and W. L. VOS, *Science* **281** (1998) 802.
4. D. WANG, R. A. CAROUS and F. CAROUS, *Chem. Mater.* **13** (2001) 364.
5. Y. XIA, B. GATES, Y. YIN and Y. LIU, *Adv. Mater.*, **12**, (2000) 531.
6. A. IMHOF and D. J. PINE, *Nature* **389** (1999) 948.
7. R. SESHADRI and F. C. MELDRUM, *Adv. Mater.* **12** (2000) 1149.
8. E. YABLONOVITCH and T. J. GMITTER, *Phys. Rev. Lett.* **63** (1989) 1950.
9. D. F. SIEVENPIPER, M. E. SICKMILLER and E. YABLONOVITCH, *ibid* **76** (1996) 2480.
10. H. YAN, C. F. BLANFORD, B. T. HOLLAND, M. PARENT, W. H. SMYRL and A. STEIN, *Adv. Mater.* **11** (1999) 1003.
11. Z. R. TIAN, W. TONG, J. Y. WANG, N. G. DUAN, V. V. KRISHNAN and S. L. SUIB, *Science* **276** (1997) 9.
12. Y. F. SHEN, R. P. ZERGER, R. N. DEGUZMAN, S. L. SUIB, L. MCCURDY, D. I. POTTER and C. L. O'YONG, *Science* **260** (1993) 511.
13. M. MAMAK, N. COOMBS and G. OZIN, *Adv. Mater.* **12** (2000) 198.
14. S. PARK, J. M. VOHS and R. J. GORTE, *Nature* **404**, (2000) 265.
15. R. CRACIUN, S. PARK, R. J. GORTE, J. M. VOHS, C. WANG and W. WORRELL, *J. Electrochem. Soc.* **146** (1999) 4019.
16. H. VERWEIJ, *Adv. Mater.* **10** (1998) 1483.
17. J. KIEFER, J. G. HILBORN and J. L. HEDRICK, *Polymer* **37** (1996) 5715.
18. D. WALSH, J. D. HOPWOOD and S. MANN, *Science* **264** (1994) 1576.
19. O. DUFAUD, E. FAVRE and V. SADTLER, *J. Appl. Polym. Sci.* **83** (2002) 967.
20. O. D. VELEV, T. A. JEDE, R. F. LODO and A. M. LENHOFF, *Nature.* **389** (1997) 447.
21. B. T. HOLLAND, L. ABRAMS and A. STERN, *Chem. Mater.* **11** (1999) 795.
22. P. JIANG, J. CIZERON, J. F. BERTONE and V. L. COLVIN, *J. Am. Chem. Soc.* **121** (1999) 7957.
23. O. D. VELEV, P. M. TESSIER, A. M. LENHOFF and E. W. KALER, *Nature* **401** (1999) 548.
24. H. YAN, C. F. BLANFORD, B. T. HOLLAND, M. PARENT, W. H. SMYRL and A. STEIN, *Chem. Mater.* **12** (2000) 1134.
25. P. YANG, T. DENG, D. ZHAO, P. FENG, D. PINE, B. J. CHMELKA, G. M. WHITESIDES and G. D. STUCKY, *Science* **282** (1998) 2244.
26. S. H. PARK and Y. XIA, *Chem. Mater.* **10** (1998) 1745.
27. A. A. ZAKHIDOV, R. H. BAUGHMAN, Z. IQBAL, C. CUI, I. KHAYRULLIN, S. O. DANTAS, J. MARTI and V. G. RALCHENKO, *Science* **282** (1998) 897.
28. Y. HOTTA, P. C. A. ALBERIUS and L. BERGSTRÖM, *J. Mater. Chem.* **13** (2003) 496.
29. K. H. RHODES, S. A. DAVIS, F. CARUSE, B. ZHANG and S. MANN, *Chem. Mater.* **12** (2000) 2832.
30. M. OHMORI and E. MATIJEVIC, *J. Colloid Interface Sci.* **150** (1992) 594.
31. A. P. PHILIPSE, M. P. B. VAN BRUGGEN and C. PATHMAMANOHARAN, *Langmuir* **10** (1994) 92.
32. H. VARMA, S. P. VIJAYAN and S. S. BABU, *J. Am. Ceram. Soc.* **85** (2002) 493.
33. F. F. LANGE, *J. Am. Ceram. Soc.* **72** (1989) 3.
34. S. BADHURI and S. B. BADHURI, *Nanostructure Mater.* **8** (1997) 755.
35. V. SERGO, G. PEZZOTTI, O. SBAIZERO and T. NISHIDA, *Act. Mater.* **46** (1998) 1701.
36. W. H. RHODES, *J. Am. Ceram. Soc.* **64** (1981) 19.
37. A. SINGHAL, L. M. TOTH, J. S. LIN and K. AFFHOLTER, *J. Am. Chem. Soc.* **118** (1996) 11529.
38. J. R. ZHANG and L. GAO, *J. Solid State Chem.* **177** (2004) 1425.
39. L. BROUSSOUS, C. V. SANTILLI, S. H. PULCINELLI and A. F. CRAIEVICH, *J. Phys. Chem.: B.* **106** (2002) 2855.
40. G. H. BODUSH and C. F. ZUKOSKI, *J. Colloid. and Inter. Sci.* **142** (1991) 1.
41. JCPDS file number 17-0923.
42. C. L. ONG, J. WANG, S. C. NG and L. M. GAN, *J. Am. Ceram. Soc.* **81**, (1998) 2624.

Received 2 June
and accepted 9 August 2005